10/5/30/89 WB (1)

UCID-21501 Part 1

A Geometric Optics Approximation to a Model of Phase-Compensated Whole-Beam Thermal Blooming

Part I. General Theory

A. K. Gautesen
J. R. Morris

September 12, 1988

Lawrence Livermore National Laboratory

This is an informal report intended primarily for internal or limited external distribution. The opinions and conclusions stated are those of the author and may or may not be those of the Laboratory.

Work performed under the auspices of the U.S. Department of Energy by the Lawrence Livermore National Laboratory under Contract W-7405-Eng-48.

Printed in the United States of America
Available from
National Technical Information Service
U.S. Department of Commerce
5285 Port Royal Road
Springfield, VA 22161

Price Code	Page Range
A01	Microfiche
Papercopy Prices	
A02	001–050
A03	051–100
A04	101–200
A05	201–300
A06	301–400
A07	401–500
A08	501–600
A09	601

A GEOMETRIC OPTICS APPROXIMATION TO A MODEL OF PHASE-COMPENSATED WHOLE-BEAM THERMAL BLOOMING*

I. GENERAL THEORY AND NUMERICAL VERIFICATION

UCID--21501-Pt.1

DE89 012893

A. K. Gautesen
Department of Mathematics
Iowa State University
Ames, Iowa

and

J. R. Morris
Lawrence Livermore National Laboratory
Livermore, CA

ABSTRACT

We develop a geometric optics series expansion approximation to a model of phase-compensated whole-beam thermal blooming of high-power laser beams. The model consists of a nonlinear medium whose thermal blooming coupling coefficient decreases exponentially with the propagation distance from the laser and whose motion relative to the laser beam is taken to be unidirectional, a Gaussian high-power intensity profile at the laser, and a collimated beam boundary condition at an exit plane that is many e-folding scale lengths from the laser. The series expansion parameter is directly proportional to Smith's geometric optics distortion parameter. [D. C. Smith, Proc. IEEE 65, 1697 (1977).] Expansion formulae are derived for both the intensity and phase at all propagation distances. The exit plane intensity profiles obtained from these formalae qualitatively agree with numerical results obtained from the wave-optics thermal blooming code FOURD, except when the FOURD results indicate that caustics are forming; quantitative agreement is also excellent, except for small differences in fine structure near the downwind edge of the beam. FOURD's return-wave phase-compensation iteration provides an estimate that the r.m.s. error in the initial phase obtained from our series approximation truncated at third-order is approximately 0.5% over the range of values we investigated.

*Work performed jointly under the auspices of the U. S. Department of Energy by Lawrence Livermore National Laboratory under contract number W-7405-ENG-48, for the U. S. Army in support of MIPR No. W31RPD-7-D4041.

1. INTRODUCTION

Herein, we study phase-compensated whole-beam thermal blooming of high-power laser beams in a medium whose thermal blooming strength decreases exponentially with propagation distance. We use a model developed by Aitken, Hayes, and Ulrich [1] which is described in Fleck, Morris, and Feit [2]. To include the effect of thermal heating on the index of refraction, this model uses linearized hydrodynamics with isobaric and steady-state approximations. An unidirectional wind is assumed.

The shape of the high-power beam at the laser is taken to be an infinite Gaussian. We seek the phase correction at the laser that will produce a collimated beam after traversing the nonlinear medium. No analytic solution to the model is known and the nonlinear index of refraction makes the existence of one unlikely. Therefore, we use a series expansion technique. First we make a geometric optics approximation to the model, justified by a large Fresnel number, and restrict our analysis to whole-beam effects. The geometric optics approximation introduces a small parameter directly proportional to Smith's [3] geometric optics distortion parameter and a solution to this approximation is found as a power series in the parameter. The terms in this series are computed using the symbolic manipulating computer program MACSYMA.

In Sec. 2, we introduce the model of Aitken, Hayes, and Ulrich [1], make the geometrical optics approximation and develop the series solution. In Sec. 3, we compare the irradiance profiles after traversing the nonlinear medium as computed by our geometrical approximation to those obtained from numerical calculations. We also use the numerical results to estimate the accuracy of the phase at the laser obtained from the geometric approximation. In the Appendix, we list the first few terms on the geometrical optics approximation to the irradiance profiles for many e-folding lengths from the laser and the phase profiles at the laser.

2. FORMULATION AND METHOD OF SOLUTION

The Basic Model

Maxwell's wave equation in the steady-state parabolic or Fresnel approximation is

$$2ik \frac{\partial E}{\partial z} = \nabla_{\perp}^2 E + k^2(n^2-1) E \tag{1}$$

where $k = 2\pi/\lambda$, λ is the wavelength of the laser, and

$$1-n^2 = -\beta \exp[-z/z_0] \int_{-\infty}^{x} |E(x_0,y,z)|^2 dx_0 \tag{2}$$

is the hydrodynamically induced change in the permitivity. In (2), z_0 is the characteristic length associated with β

$$\beta = \frac{2\alpha}{C_p \; Tv} \frac{dn}{d\rho} \tag{3}$$

where α is absorption coefficient, $\frac{dn}{d\rho}$ is the density refractive coefficient, C_p is the heat capacity of the air, T is the ambient air temperature, and v is the wind speed all evaluated at z=0. The wind velocity is taken to be in the positive x-direction. At the laser the intensity of the beam is taken to be the Gaussian

$$|E(x,y,0)|^2 = 2P \exp[-2(x^2+y^2)/a^2]/(\pi a^2) \tag{4}$$

where P is the power in the beam and a is its effective radius.

It is convenient to introduce the following scaling in (1), (2), and (4):

$$(x,y) = a(\bar{x},\bar{y})/\sqrt{2} \tag{5}$$

$$z = z_0\bar{z} \tag{6}$$

$$E = [2P/(\pi a^2)]^{1/2} \bar{E} \tag{7}$$

The result is

$$2iN_F \frac{\partial E}{\partial z} = \nabla_\perp^2 E - 4\delta N_F^2 e^{-z} \int_{-\infty}^{x} |E(x_0,y,z)|^2 \, dx_0 \, E \tag{8}$$

$$|E(x,y,0)|^2 = \exp[-x^2 - y^2] \tag{9}$$

where $N_F = ka^2/2z_0$ is the Fresnel number,

$$\delta = \beta z_0^2 P/(2^{1/2}\pi a^3) = \sqrt{\pi}\, N_\lambda/N_F, \tag{10}$$

and N_λ is the total peak optical path difference (in waves) due to thermal blooming when intensity reshaping and transmission losses are ignored. In (8), (9), and the sequel we have dropped the overbars on E, x, y, and z.

Geometric Optics Approximation

Let

$$E = A^{1/2} \exp[-i2\delta N_F \phi] \tag{11}$$

where $A \geq 0$ and ϕ is real. Then after multiplying (8) by $\exp[i2\delta N_F \phi]$, the imaginary and real parts become

$$\frac{\partial A}{\partial z} + 2\delta \nabla_\perp \phi \cdot \nabla A + 2\delta A \nabla_\perp^2 \phi = 0 \tag{12}$$

$$\frac{\partial \phi}{\partial z} + e^{-z} \int_{-\infty}^{x} A(x_0,y,z) \, dx_0 + \delta |\nabla_\perp \phi|^2 = (4\delta N_F^2 A^{1/2})^{-1} \nabla_\perp^2 (A^{1/2}) \tag{13}$$

The geometric optics limit of (13) is the $N_F \to \infty$ limit. For cases of interest $N_F > \pi 10^3$ and $\delta > 0.006$, so we have

$$\delta N_F^2 \gg 1 \tag{14}$$

Therefore we approximate (13) by ignoring the right-hand side, thus

$$\frac{\partial\phi}{\partial z} + e^{-z} \int_{-\infty}^{x} A(x_0,y,z)dx_0 + \delta|\nabla_\perp\phi|^2 = 0 \tag{15}$$

Upon substitution of (11) into (9) we find that A satisfies the initial condition

$$A(x,y,0) = \exp[-x^2 - y^2] \tag{16}$$

The condition that the beam is collimated in space becomes

$$\phi(x,y,\infty) = 0 \tag{17}$$

Thus, we seek the solutions to (12) and (15) that satisfy (16) and (17).

Geometric Optics Solution

At power levels of interest we can assume,

$$\delta << 1 \tag{18}$$

Therefore, we take

$$A = \sum_{m=0}^{\infty} \delta^m \sum_{n=0}^{m} A_m^n(x,y)\, e^{-nz} \tag{19}$$

$$\phi = \sum_{m=0}^{\infty} \delta^m \sum_{n=0}^{m} \phi_m^n(x,y)\, e^{-(n+1)z} \tag{20}$$

Upon substitution of (19) and (20) into (12), and setting the coefficients of the terms $\delta^m e^{-nz}$ equal to zero yields

$$\frac{\partial A_m^0}{\partial z} = 0 \quad , \quad m = 0,\ 1,\ \ldots \tag{21}$$

$$A_{m+1}^{n+1} = \frac{2}{n+1} \sum_{k=0}^{m} \sum_{\ell=\max(0,k+n-m)}^{\min(k,n)} \nabla_\perp \cdot [A_{m-k}^{n-\ell} \nabla_\perp \phi_k^\ell] \; ,$$

$$n = 0, 1, \ldots, m, \qquad m = 0, 1, \ldots \tag{22}$$

Since A_m^0 is only a function of x and y, (21) is automatically satisfied. These functions are chosen to satisfy the initial condition (16). Thus,

$$A_0^0 = \exp(-x^2 - y^2) \tag{23}$$

$$A_{m+1}^0 = -\sum_{n=0}^{m} A_{m+1}^{n+1} \; , \quad m = 0, 1, \ldots \tag{24}$$

Next substitution of (19) and (20) into (15) and setting the coefficients of the terms $\delta^m e^{-(n+1)z}$ equal to zero yields

$$\phi_0^0 = \int_{-\infty}^{x} A_0^0(x_0,y) \, dx_0 \tag{25}$$

$$\phi_{m+1}^0 = \int_{-\infty}^{x} A_{m+1}^0(x_0,y)dx_0 \quad , \quad m = 0, 1, \ldots \tag{26}$$

$$\phi_{m+1}^{n+1} = \frac{1}{n+2} \left[\int_{-\infty}^{x} A_{m+1}^{n+1} (x_0,y)dx_0 \right.$$

$$\left. + \sum_{k=0}^{m} \sum_{\ell=\max(0,k+n-m)}^{\min(k,n)} \nabla_\perp A_{m-k}^{n-\ell} \cdot \nabla_\perp \phi_k^\ell \right] ,$$

$$n = 0, 1, \ldots, m, \qquad m = 0, 1, \ldots \tag{27}$$

The remaining condition (17) is automatically satisfied by (20).

In summary, A_0^0 and ϕ_0^0 are defined by (23) and (25), respectively. Then for fixed m, A_{m+1}^j and ϕ_{m+1}^j for j = 0, 1, ..., m+1 are recursively defined in terms of known quantities by (22), (24), (26), and (27). These computations have been performed using the symbolic manipulating program MACSYMA.

The quantities of physical interest are the irradiance profile many e-folding lengths from the laser

$$A(x,y,\infty) = \sum_{m=0}^{\infty} \delta^m A_m^0(x,y) \tag{28}$$

and the phase profile at the laser

$$\phi(x,y,0) = \sum_{m=0}^{\infty} \delta^m \sum_{n=0}^{m} \phi_m^n(x,y) \tag{29}$$

In the Appendix, we list the various terms of $A_m^0(x,y)$ and $\sum_{n=0}^{m} \phi_m^n(x,y)$,

for m = 1, 2.

3. COMPARISON WITH WAVE-OPTICS CALCULATIONS

To evaluate the accuracy of the analytic model, including the impact of omitting diffraction and transmission loss due to absorption, we compare its results to those obtained from our wave-optics thermal blooming code, FOURD. For initial conditions in the FOURD calculations we use the z = 0 phase given by Eq. (29) truncated at m = 3 and multiplied by $\delta\ N_F$, as in Eq. (11), plus a Gaussian intensity profile. Figure 1 shows these initial phase profiles as contour plots with a one wave level separation and a base zero-wave level (not shown) far upwind of the high-power beam. We evaluate the FOURD code results for a propagation path length of $5z_0$, a Fresnel number N_F = 741 (at z_0), and a 0.02 optical depth due to absorption. Finally, we use a steady-state return-wave phase-compensation iteration to estimate how close the analytic model came to a "best correction." (The above choice of path length, Fresnel number, and optical depth is our compromise between modeling the total absorption optical depth, staying at parameter values for which geometric optics is an excellent approximation, and modeling interesting laser systems.)

Figure 2 shows the extent to which the near-field intensity analytic results given by Eq. (28) truncated at $m = 4$ agree with the corresponding results obtained from FOURD at the end of the propagation path; the results are displayed as contour plots drawn with levels at the peak intensity and at 0.9, 0.8, ... thereof. The analytic model reproduces the qualitative behavior of and also achieves reasonable quantitative agreement with the FOURD results, except at the largest δ value. The principal quantitative difference is the resolution of fine structure near the downwind edge of the beam; this difference increases monotonically with increasing δ, and is probably due to truncation of the series in Eq. (28). At the largest δ value the analytic model's intensity profile has two regions of negetive values (inside the open U-shaped contours above and below the symmetry axis), indicating that its region of validity for truncation at $m = 4$ has been exceeded. The corresponding wave-optics result shows evidence of two caustics in the downwind fine structure.

Table 1 characterizes the accuracy of the analytic model in several ways. The Strehl ratio in column 2 approximately measures extent to which the analytic model has produced a flat phase at the end of the propagation path. The change in the Strehl ratio achieved with a return-wave phase-compensation iteration measures the combined effects of truncating the analytic phase series at $m = 3$ and of differences between the equations solved by the analytic model and by FOURD. Column 5 contains an r.m.s. phase difference, $\delta\Phi$, obtained by equating the ratio of these two Strehl ratios to $\exp[-(2\pi\delta\Phi)^2]$. These differences are approximately 0.5% of optical path difference (OPD) due to thermal blooming given in column 4, and some of this small difference is due to the finite optical depth and finite path length in the FOURD calculations (discussed below).

In the FOURD calculations, we used a constant $0.25 \cdot z_0$ propagation step and a square mesh whose width was 4 times the e^{-2} diameter of the Gaussian high-power beam. For $\delta = 0.0221$ and 0.0442 we used a 256 by 256 mesh; for $\delta = 0.0331$ and 0.0662 we used a 512 by 512 mesh. The return-wave phase-compensation iteration employs a wave-optics algorithm starting with a collimated tenth-power super-Gaussian beacon at $z = 5z_0$ whose diameter at e^{-1} is approximately 2.3 times the e^{-2} diameter of the Gaussian high-power laser beam at $z = 0$ and whose wavelength equaled that of the high-power laser beam.

For the highest δ value the maximum spectral density at the Nyquist boundary is approximately 10^{-7} times the peak spectral density, which usually indicates that the calculation is free of spectral aliasing. Nevertheless, the downwind fine structure above and below the two intensity maxima closest to the symmetry axis is suspiciously reminiscent of such aliasing and may be an artifact of inadequate resolution. All the other calculations are definitely free of aliasing.

We have examined the effects of various differences between the equations of the analytic model and those solved by FOURD. The effect of the finite Fresnel number, $N_F = 741$, was evaluated by running the $\delta = 0.0221$ and 0.0331 cases at $N_F = 1482$. The effect of finite optical depth due to absorption was estimated by running the $\delta = 0.0331$ case with an optical depth a factor of 10^{-3} smaller. For both the increased Fresnel number and the smaller optical depth cases the intensity results at the end of the propagation path were indistinguishable from those in Figure 2.

Table 1. Measures of the accuracy of the analytic model obtained from FOURD calculations at $N_F = 741$.

	Strehl ratios for		Estimated phase (waves)	
δ	Analytic Phase	One return-wave iteration	peak OPD from ϕ_0^0	r.m.s. difference from return-wave
0.0221	0.961	0.984	4.6	0.024
0.0331	0.925	0.974	6.9	0.036
0.0442	0.884	0.950	9.2	0.043
0.0662	0.709	0.758	13.9	0.041

REFERENCES

[1] A. H. Aitken, J. N. Hayes, and P. B. Ulrich, NRL Report 7293 (1971).

[2] J. A. Fleck, Jr., J. R. Morris, and M. D. Felt, "Time-dependent propagation of high energy laser beams through the atmosphere," Appl. Phys. 10, pp. 129 (1976).

[3] D. C. Smith, "High-power laser propagation: thermal blooming," Proc. IEEE 65, pp. 1679 (1977).

APPENDIX

In this Appendix, we give the first few terms appearing in the series in (28) and (29). We write

$$A_m^0 = \sum_{n=0}^{m} B_m^n(x)\ y^{2n}\ \exp[-(m+1)y^2]$$

$$\Psi_m = \sum_{n=0}^{m} \psi_m^n(x)\ y^{2n}\ \exp[-(m+1)y^2]$$

where

$$\Psi_m = \sum_{n=0}^{m} \phi_m^n(x,y)$$

Then

$$B_1^0 = e\{2pf + 2p + 8xe\}$$

$$B_1^1 = -8pe\{f+1\}$$

$$B_2^0 = e\{10p^2f^2 + 20p^2f + 28pxef + 10p^2 + 28pxe + 108x^2e^2 - 38e^2\}$$

$$B_2^1 = -e\{114(pf)^2 + 228p^2f + 120pxef + 114p^2 + 120pxe - 96\ e^2\}$$

$$B_2^2 = 108p^2e\ \{f^2 + 2f + 1\}$$

$$\psi_1^0 = -\frac{1}{2}\ e^2 + \frac{1}{4}\ p^2(f+1)^2$$

$$\psi_1^1 = -\frac{1}{2}\ p^2(f+1)^2$$

$$\Psi_2^0 = \frac{4}{3}\{-2xe^3 - pe^2(1+f) + \frac{1}{2}p^3(1+f)^3 - 3^{-1/2}p(1+f_3)\}$$

$$\Psi_2^1 = \frac{4}{3}p\{2e^2(1+f) - 3p^2(1+f)^3 + 2(3)^{1/2}(1+f_3)\}$$

$$\Psi_2^2 = \frac{8}{3}p^3(1+f)^3$$

Here

$$e = \exp(-x^2)$$

$$f = \frac{2}{\pi^{1/2}}\int_0^x e^{-t^2}\,dt = \mathrm{Erf}(x)$$

$$f_3 = \mathrm{Erf}(x3^{1/2})$$

$$p = \pi^{1/2}$$

FIGURE CAPTIONS

Figure 1 Initial phase profiles predicted by the geometric optics series expansion truncated at third order. The normalized values of the expansion model have been scaled to physical phase values in waves for a case with a Fresnel number of 741. The contour separation is one wave and the base contour (not visible) is at the ambient optical path which occurs infinitely far to the left on these plots.

Figure 2 Comparison of path end near-field intensities. The FOURD wave-optics numerical results are at $5z_0$, while the series expansion results are at infinity. The contour levels in each plot are at the peak intensity of that plot and 0.9, 0.8, ... times thereof.

Analytic model initial phase to $O(\delta^3)$ for N_F = 741

δ = 0.0221 0.0331 0.0442 0.0663

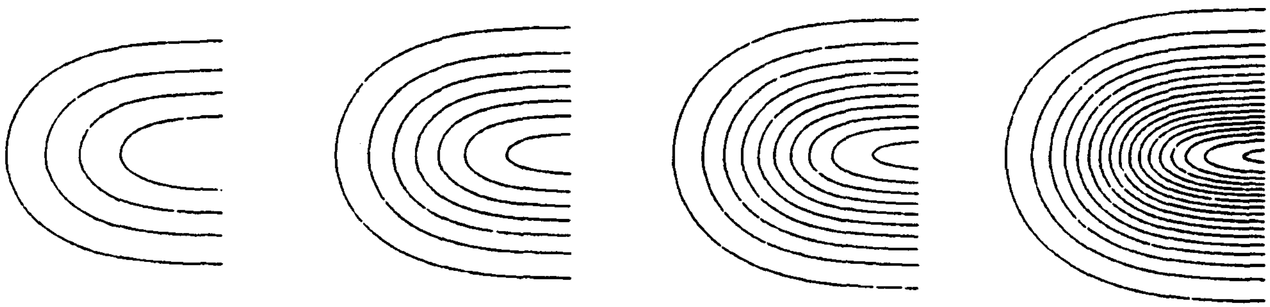

Figure 1

MPJM 02-88-27

Comparison of analytic model to wave-optics calculation — end of path intensities

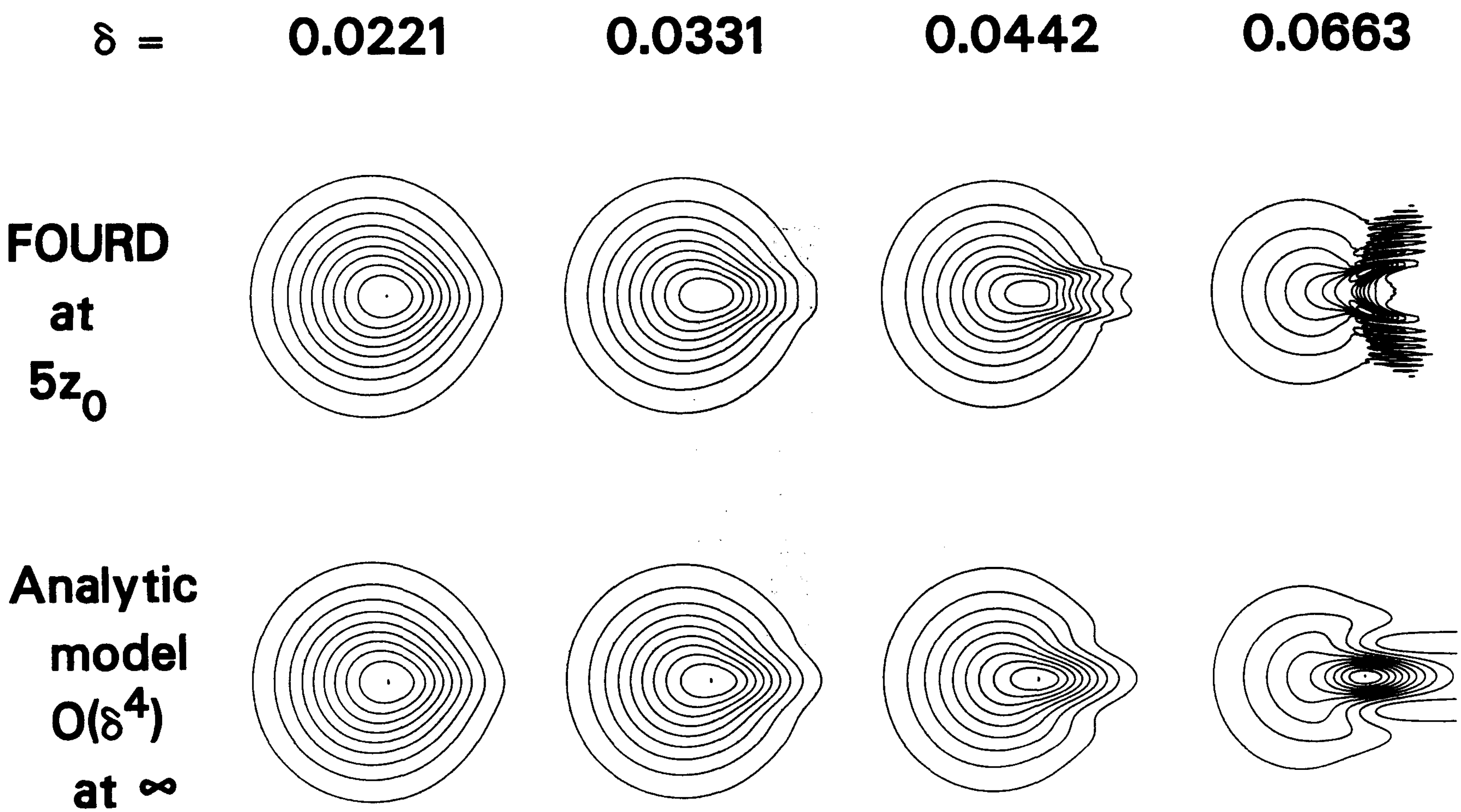

Figure 2

MPJM 02-88-26